Appl Phys B (2011) 103:701–706
DOI 10.1007/s00340-010-4292-3

Applied Physics B
Lasers and Optics

Surface plasmon resonance biosensing by electro-optically modulated attenuated total reflection

T.-J. Wang · C.-C. Cheng · S.-C. Yang

Received: 15 July 2010 / Revised version: 26 October 2010 / Published online: 23 November 2010

Abstract This study presents a surface plasmon resonance biosensing technique based on electro-optically modulated attenuated total reflection. The initial wavevector of the light for exciting surface plasmons is specified by setting the incident angle and is then modulated by electro-optic effect. The light power which is attenuated-total-reflected from the metal/dielectric interface is correspondingly electro-optically modulated. Its variation with the applied voltage is utilized to determine the analyte concentration. In the biosensing process, the incident angle determines the initial position of the operation point and thus the detection sensitivity. The presented technique has the features of resolution tunability and sensitivity tunability under various base indices of sensing layer or analyte solution for optimal operation. In this work, the effects of the incident angle, the Au-film thickness, and the ridge width on the detection sensitivity are also discussed.

1 Introduction

Optical sensing by surface plasmon resonance (SPR) has many attractive features, such as high detection sensitivity, no need of fluorescent labeling, and real-time sensing [1]. SPR phenomenon, which is the result of coupling input light to surface plasmons, occurs when the component of the input light wavevector along the metal/dielectric interface equals the propagation constant of surface plasmons. This phase matching condition can be achieved by tuning the wavevector of input light in the couplers such as prism coupler [2–5], waveguide coupler [6, 7], and grating coupler [8]. Among three couplers, the prism coupler using attenuated total reflection (ATR) on the metal/dielectric interface is the most popular and widely used in the sensing/biosensing application. In prism coupler, the wavevector of the light for exciting surface plasmons is tuned by varying the incident angle [2] or the light wavelength [3]. Various sensing improvements, such as simultaneous excitation of two plasmon modes [2], wavelength division multiplexing [3], colloidal Au-enhanced SPR [4], and SPR imaging [5], have been proposed.

Previously, electro-optically modulated SPR waveguide biosensors on $LiNbO_3$ are presented [9]. The effective index of the optical field propagating in the waveguide is tuned by electro-optic effect to vary the phase matching condition. The output power variation caused by electro-optic modulation is utilized to determine analyte concentration. In order to obtain the maximal detection sensitivity under various sensing environments, the initial wavevector of the input light needs to be varied in a large range for achieving optimal operation. However, for the waveguide biosensor on $LiNbO_3$, the effective index (or the light wavevector) of the optical field only can be slightly varied due to the limitation of waveguide fabrication method and waveguide operation principle. The detection sensitivity of such waveguide biosensors cannot be tuned under various base indices of sensing layer or analyte solution for optimal operation. In this work, we present a new SPR biosensing technique by electro-optically modulated attenuated total reflection. The input light for exciting surface plasmons is incident on the semispherical prism and is then attenuated-total-reflected on the metal/dielectric interface. The initial light wavevector can be varied in a large range simply by changing the in-

T.-J. Wang (✉) · C.-C. Cheng · S.-C. Yang
Institute of Electro-Optical Engineering, National Taipei University of Technology, No. 1, Sec. 3, Chung-Hsiao E. Road, 10608 Taipei, Taiwan, R.O.C.
e-mail: f10939@ntut.edu.tw
Fax: +886-2-87733216

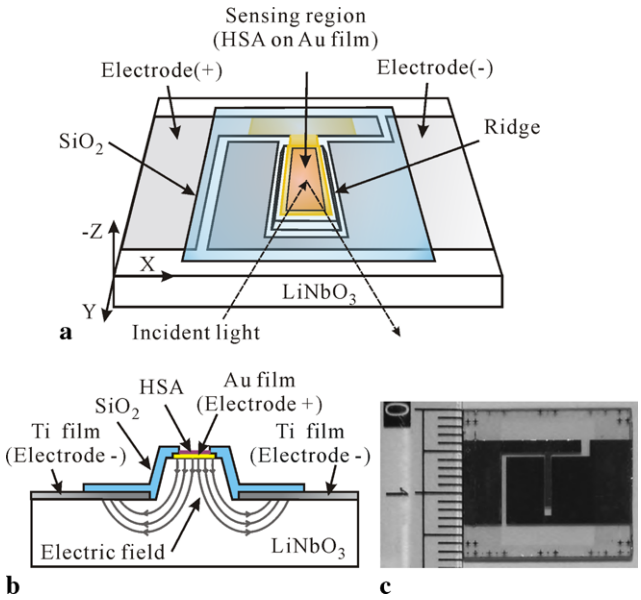

Fig. 1 (**a**) Device structure of the presented SPR biosensor; (**b**) its cross-section view; (**c**) photograph of the finished SPR biosensor

cident angle. This feature makes the proposed SPR biosensing technique owns the in-situ detection sensitivity tunability under various sensing environments for optimal operation.

2 Biosensor design, fabrication and measurement

2.1 Biosensor design

Figure 1(a) shows a SPR biosensor produced on z-cut $LiNbO_3$ using three-electrode structure. An Au film coated over the sensing region is used to support surface plasmon and as central electrode. Two Ti films placed on two sides of the ridge structure are used as side electrodes, as shown in Fig. 1(b). Human serum albumin (HSA) is self-assembled over the Au film as the sensing layer. The analyte is beta-blocker (alprenolol), which is an effective remedy for heart disease. The binding of HSA with beta-blocker results in the index increase of the sensing layer. For exciting surface plasmons, the p-polarized light is incident on the (1:$LiNbO_3$/2:Au-film/3:sensing-layer/4:analyte-solution) four-layer structure. The phase matching condition is expressed as the equivalence of the component of the input light wavevector along the Au/$LiNbO_3$ interface k_x and the propagation constant of surface plasmons k_{sp}:

$$k_x = \frac{2\pi}{\lambda} n_1(\theta) \cdot \sin\theta = k_{sp} \tag{1}$$

where λ is the light wavelength in vacuum, θ is the incident angle, n_i is the complex index of layer i. Due to the birefringence of $LiNbO_3$, the index for p-polarized light varies with θ in the manner:

$$n_1(\theta) = \frac{n_o n_e}{\sqrt{n_o^2 \sin^2\theta + n_e^2 \cos^2\theta}} \tag{2}$$

The n_o and n_e are ordinary and extraordinary indices, and can be electro-optically modulated according to: $n_o = n_{o,0} - (1/2) \cdot r_{13} \cdot n_{o,0}^3 \cdot E_Z$ and $n_e = n_{e,0} - (1/2) \cdot r_{33} \cdot n_{e,0}^3 \cdot E_Z$, where $n_{o,0}$ and $n_{e,0}$ are the indices without applying electric field, r_{13} and r_{33} are the electro-optic coefficients, E_z is the z-component of the induced electric field. The electric field is produced by applying a voltage on the three-electrode structure. The design of the center electrode placed on the ridge structure has two effects; one is to enhance the intensity of the z-component of the induced electric field and the other is to provide the appropriate electro-optic index change distribution for effectively modulating the wavevector component. The reflectivity of the p-polarized light incident on the four-layer structure is expressed as

$$R = \left| \frac{r_{12} + r_{12} \cdot r_{23} \cdot r_{34} \exp(2ik_{z3}d_3) + [r_{23} + r_{34} \exp(2ik_{z3}d_3)] \exp(2ik_{z2}d_2)}{1 + r_{23} \cdot r_{34} \exp(2ik_{z3}d_3) + r_{12} \cdot [r_{23} + r_{34} \exp(2ik_{z3}d_3)] \exp(2ik_{z2}d_2)} \right|^2 \tag{3}$$

where d_i is the thickness of layer i, and the reflection coefficients r_{ij} are given as

$$r_{ij} = (z_i - z_j)/(z_i + z_j) \tag{4}$$

where $z_i = n_i^2/k_{zi}$, k_{zi} is the z-component of the wavevector in the ith layer and is given as

$$k_{zi} = k_0 \left(n_i^2 - n_1^2 \sin^2\theta\right)^{1/2} \tag{5}$$

where k_0 is the wavevector in vacuum. The output power variation with the incident angle and the index of the sensing layer can be theoretically calculated according to (2)–(5).

Figure 2(a) shows the shift of the angular SPR curve with the index of the sensing layer. This curve has the same shape as the measured one. As the analyte concentration (or the index of the sensing layer) increases, the angular SPR curve shifts toward the right side (from the dashed one to the solid one in Fig. 2(a)). Consider the incident angle is fixed at θ

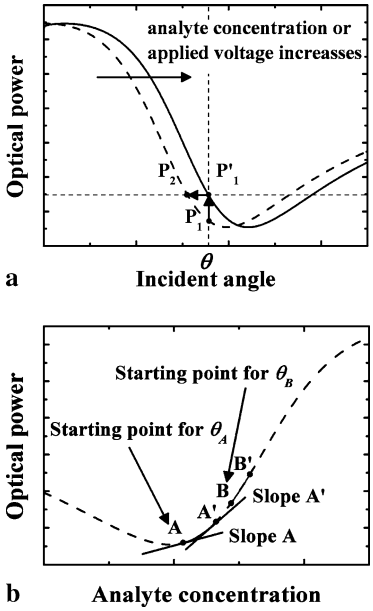

Fig. 2 Schematic diagram of (**a**) the shift of the angular SPR curve as the analyte concentration increases (the *dashed curve* is the original one, the *solid curve* corresponds to the one with the increase of analyte concentration); (**b**) the dependence of the output power on the analyte concentration for the incident angle θ_A and θ_B

which is on the left side of the SPR angle. The output power at the fixed θ increases with the analyte concentration, corresponding to the movement of the operation point from P_1 to P_1'. The effect of increasing analyte concentration can be viewed as moving the operation point along the original angular SPR curve from P_1 to P_2. Figure 2(b) shows the dependence of the output power on the analyte concentration. The point A (or B) corresponds to the condition for the incident angle at θ_A (or θ_B) and zero analyte concentration. When the analyte concentration increases, the operation point is moved from A to A'. The corresponding slope of tangent line for the operation point $A \rightarrow A'$ becomes larger. Due to its concentration dependence, the slope of tangent line can be used to determine analyte concentration. Besides, the slope increase for moving the operation point from A to A' is larger than that from B to B'. It means that the detection sensitivity measured at θ_A is larger than that at θ_B. Therefore, the detection sensitivity depends on the initial operation point and can be tuned by changing the incident angle. Increasing applied voltage has the same effect as increasing the incident angle. It produces the index change in $LiNbO_3$ and thus the increase of output power. When the index change is small, the relation between output power and applied voltage is approximately linear. The regression slope of this relation is used to approximate the slope of tangent line of the power-versus-concentration curve for determination of analyte concentration.

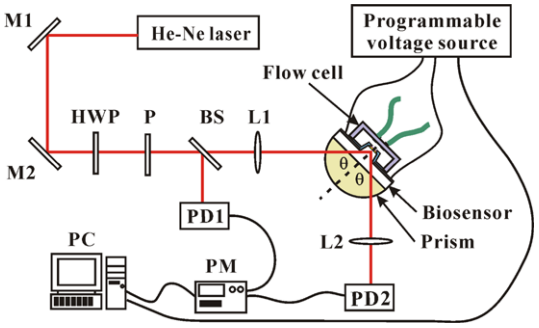

Fig. 3 Measurement setup (M1, M2: mirror, HWP: half-wave plate, P: polarizer, BS: beam splitter, L1, L2: lens, PD1, PD2: photodetector, PM: power meter, PC: personal computer)

2.2 Fabrication process

The biosensor is produced as follows. First, a patterned 120 nm-thick Cr film used as etching mask is formed on the $-z$ face of $LiNbO_3$ substrate by optical lithography and RF magnetron sputtering. Then the substrate is immersed in the diluted HF solution (1:2) for 10 hours to obtain a 5 μm etching depth. After removing the Cr film, a 30 nm-thick Au film and a 300 nm-thick Ti film with individual patterns shown in Fig. 1(a) are sequentially produced on the substrate surface by thermal evaporation and RF magnetron sputtering. To avoid short circuit of electrodes caused by analyte solution injected during the biosensing measurement, a 300 nm-thick SiO_2 film with the opening on the sensing region is deposited by RF magnetron sputtering. Next, HSA is self-assembled on the Au surface on the sensing region by chemical modification method [9]. Finally, it is stored at 4°C before use. The photograph of the finished SPR biosensor is shown in Fig. 1(c). The beta-blocker aqueous solutions are used as analyte solutions. They are prepared by using the mixture of acetonitrile and distilled water (1:9) as solvent and have the concentrations of $0 \sim 5$ ppm.

2.3 Biosensing measurement

Figure 3 shows the measurement setup. The laser light at the wavelength of 632.8 nm passes through a half-wave plate and a polarizer to adjust for p-polarization at the input of the prism coupler. The laser light is split into the reference beam and the measurement beam by a R8/T92 beam splitter. The measurement beam is focused by the lens and incident on the N-SF66 ($n = 1.9142$) semispherical prism. The biosensor is attached on the flat face of the prism with the gap filled by the index-matching liquid ($n = 1.8$, Cargille Labs). The measurement beam reflected from the Au/$LiNbO_3$ interface is collected by the lens. Finally, the measurement beam and the reference beam are, respectively, received by photodetectors for optical power measurement. The power ratio is defined as the ratio of the power of the measurement beam

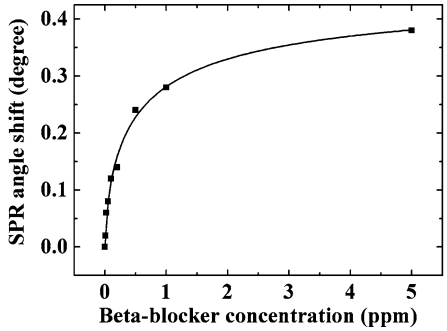

Fig. 4 Dependence of the SPR angle shift on the beta-blocker concentration for the biosensor with a 30 nm-thick Au-film

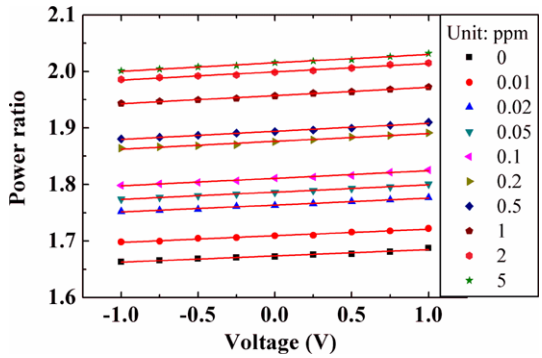

Fig. 5 Dependence of the power ratio on the applied voltage for the beta-blocker concentration $C = 0 \sim 5$ ppm

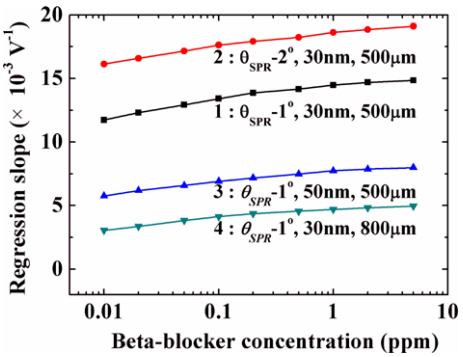

Fig. 6 Dependence of the regression slope on the beta-blocker concentration for four SPR biosensors with parameters (θ_i, t_{Au}, w_{rdg})

to that of the reference beam. The biosensing measurement starts after the beta-blocker solution is injected into the flow cell for five minutes. When the voltage is applied on the electrodes of the SPR biosensor, the powers of the measurement beam and the reference beam are measured. The processes of voltage scanning and power measurement are controlled by personal computer using the Labview program. The analyte concentration is determined by measuring the regression slope of the relation between the power ratio and the applied voltage at the fixed incident angle. Before each new measurement, the sensing layer is regenerated by injecting pure acetonitrile into a flow cell to disrupt the force that binds beta-blocker to HSA.

3 Results and discussions

3.1 Conventional ATR measurement

The dependence of output power on the incident angle is first measured for determining the SPR angle. For the beta-blocker concentration $C = 0$ ppm, the SPR angle for the biosensor with a 30 nm-thick Au-film and a 500 μm-wide ridge is $\theta_{\mathrm{SPR}} = 43.34°$. Figure 4 shows the dependence of the SPR angle shift on the beta-blocker concentration for $C = 0 \sim 5$ ppm. With the increase of the beta-blocker concentration, the SPR angle increases initially rapidly in a linear manner. The detection sensitivity in the linear detection range $C = 0 \sim 0.05$ ppm is 1.571 degree/ppm. Further increase of beta-blocker concentration results in the SPR angle approaching a constant value. For the angular resolution of 0.001 degree, the detection resolution is 6.365×10^{-4} ppm.

3.2 Electro-optically modulated ATR measurement

In order to demonstrate the effect of electro-optic modulation, the dependence of output power ratio on the applied voltage at the specific incident angle is measured. Figure 5 shows the results for the biosensor at the incident angle $\theta_i = 42.34°(= \theta_{\mathrm{SPR}} - 1°)$ for $C = 0 \sim 5$ ppm. The power ratio increases linearly with the applied voltage and has an average correlation coefficient 0.9932. Besides, the output power at the same voltage increases with the beta-blocker concentration. This result is consistent with the description in the previous section.

The sensing performance is related to the incident angle θ_i, the Au-film thickness t_{Au}, and the ridge width w_{rdg}. Figure 6 shows the dependence of the regression slope on the beta-blocker concentration for four SPR biosensors with parameters (θ_i, t_{Au}, w_{rdg}). As the beta-blocker concentration increases, the regression slope becomes larger and its increase rate is reduced at larger concentration. For real concentration measurement, it is necessary to establish the calibration curve. Because the relation between the regression slope and the beta-blocker concentration is nonlinear, a best-fitted calibration function for this relation is sough to have good coincidence with the calibrated data. The measured concentration value can be inferred from the calibration function. Since the turning point is located around $C = 0.1$ ppm, the detection sensitivity is calculated in the range $C = 0 \sim 0.1$ ppm.

The effect of the incident angle on the sensing performance is manifested by comparing Curve 1 and 2, which correspond to $\theta_i = (\theta_{\mathrm{SPR}} - 1°)$ and $(\theta_{\mathrm{SPR}} - 2°)$.

Their detection sensitivities are 2.115×10^{-2} and 1.807×10^{-2} V^{-1} ppm^{-1}, respectively. The initial operation point for $\theta_i = (\theta_{SPR} - 1°)$ and $(\theta_{SPR} - 2°)$ are equivalent to the operation points A and B in Fig. 2(b). As described previously, because there is a larger slope change of tangent line near the operation point A, the SPR biosensing at $\theta_i = (\theta_{SPR} - 1°)$ has higher detection sensitivity.

To reveal the effect of Au-film thickness, the biosensors with $t_{Au} = 30$ nm and 50 nm are measured at $\theta_i = (\theta_{SPR} - 1°)$ with the results corresponding to Curve 1 and 3 in Fig. 6. The detection sensitivities for $t_{Au} = 30$ nm and 50 nm are 2.115×10^{-2} and 1.426×10^{-2} V^{-1} ppm^{-1}. In the SPR sensing using glass prism ($n \approx 1.5$), a 50 nm-thick Au-film is often used. Since $LiNbO_3$ ($n \approx 2.2$) has a higher index than glass, the penetration depth of the evanescent field caused by total reflection on the Au/$LiNbO_3$ interface is smaller than that on the Au/SiO_2 interface. Hence, the used Au-film thickness is required to be reduced such that sufficient evanescent field extends to the Au/sensing-layer interface to sense the index change of the sensing layer. It is the reason that the SPR biosensor with $t_{Au} = 30$ nm has higher detection sensitivity.

The effect of ridge width on the sensing performance is demonstrated by comparing the sensing properties of the SPR biosensors with $w_{rdg} = 500$ μm and 800 μm. Their sensing properties correspond to Curve 1 and 4 in Fig. 6 and their detection sensitivities are 2.115×10^{-2} and 1.394×10^{-2} V^{-1} ppm^{-1}. The cause of higher detection sensitivity for $w_{rdg} = 500$ μm is that narrower ridge facilitates to produce stronger electric field and appropriate index distribution for effectively modulating the light wavevector. Among these four SPR biosensors, the biosensor with $\theta_i = 42.34°$, $t_{Au} = 30$ nm, and $w_{rdg} = 500$ μm, has the highest detection sensitivity of 2.115×10^{-2} V^{-1} ppm^{-1}. Because the breakdown electric field of $LiNbO_3$ is about 10 V/μm, the breakdown voltage for the electrode gap of 50 μm is about 500 V. For the resolution of power ratio of 0.001 and ±50 V voltage scanning, the detection resolution is 4.728×10^{-4} ppm. Higher detection resolution can be obtained by using higher power-ratio resolution and larger scanning voltage.

3.3 Discussion

The conventional SPR sensing by angle interrogation requires bulky motorized rotation stages to vary the incident angle and position the photodetector for receiving the reflected light. The overall system is large and its setup requires higher cost. Besides, its sensing performance, such as detection resolution and measurement time, is limited by rotation resolution, rotation speed, and noise from mechanical vibration. The presented SPR biosensing technique utilizes the voltage scanning, instead of mechanical rotation, to vary the component of the light wavevector along the interface. Voltage scanning combining with photodetectors for measuring optical power constitutes an all-electronic measurement, which possesses the advantageous features, such as high precision, high resolution, high stability, high measurement speed, and low instrument cost. Besides, the presented SPR biosensing technique simultaneously possesses the features of resolution tunability and sensitivity tunability. During the SPR biosensing measurement, as the change of the output power is too small to be measured, increasing the applied voltage can enlarges the power change such that the power change becomes distinguishable. Thus the detection resolution can be enhanced by increasing the applied voltage. The detection sensitivity of the SPR biosensor in general depends on the base index of the sensing layer or analyte solution. The presented technique can tune the detection sensitivity under various sensing environments for optimal operation by changing the incident angle of the input light.

4 Conclusions

In this work, we present a new SPR biosensing technique based on electro-optically modulated attenuated total reflection. The initial wavevector of the light for exciting surface plasmons is specified by setting the incident angle and is then modulated by the electro-optic effect. The analyte concentration can be determined by measuring the regression slope of the relation between the output power and the applied voltage. The detection sensitivity can be tuned by changing the incident angle of the input light to suit various sensing environment. The effects of the Au-film thickness and the ridge width on the sensing performance are also discussed. A thinner Au film than that used in glass material is required here to have sufficient extension of the evanescent field to the Au/sensing-layer interface. Narrower ridge width facilitates the enhancement of the electric field intensity to achieve high detection sensitivity. The presented SPR biosensing technique possesses the unique features of in-situ resolution tunability and sensitivity tunability for optimal operation.

Acknowledgements The authors would like to thank the support from National Science Council, Taipei, Taiwan, Republic of China under the contract No. NSC97-2221-E-027-009-MY3.

References

1. J. Homola, Chem. Rev. **108**, 462 (2008)
2. S. Patskovsky, A.V. Kabashin, M. Meunier, J.H.T. Luong, Appl. Opt. **42**, 6905 (2003)
3. J. Dostalek, H. Vaisocherova, J. Homola, Actuators, B Chem. **108**, 758 (2005)

4. L.A. Lyon, M.D. Musick, J.J. Natan, Anal. Chem. **70**, 5177 (1998)
5. K. Johansen, H. Arwin, I. Lundstrom, B. Liedberg, Rev. Sci. Instrum. **71**, 3530 (2000)
6. J. Shibayama, IEEE Photonics Technol. Lett. **22**, 643 (2010)
7. Y.-C. Lin, W.-H. Tsai, Y.-C. Tsao, J.-K. Tai, IEEE Photonics Technol. Lett. **20**, 1287 (2008)
8. B.K. Singh, A.C. Hillier, Anal. Chem. **80**, 3803 (2008)
9. T.-J. Wang, W.-S. Lin, F.-K. Liu, Biosens. Bioelectron. **22**, 1441 (2007)